Slope Stability 2007 — Y. Potvin (ed)

https://papers.acg.uwa.edu.au/p/708_2_Linero/

Geotechnical Characterisation of Waste Material in Very High Dumps with Large Scale Triaxial Testing

S. Linero *SRK Consulting, Chile*

C. Palma *SRK Consulting, Chile*

R. Apablaza *Codelco Andina Division, Chile*

Abstract

Large scale, open pit copper mining in Chile involves the mobilization of large amounts of waste material from the pit to areas specifically prepared to store this material. The challenge faced by some mines in the Andean mountain range is the lack of available space for waste dumps given the steepness of the typical mountainous topography. Because of this there is an ever more urgent need to design very high dumps that are unprecedented in the world.

Usually verification of the stability of waste dumps does not pose a significant difficulty. However, in the case of deposits that can be hundreds of metres high at the face, such as those planned by Codelco´s Andina Division, it becomes necessary to have detailed knowledge of the geomechanical behaviour of the material. In general, the studies in characterisation of coarse granular material have been done in relation to the construction of rockfill dams. Waste dumps, as opposed to dams, are generally built simply by overturning truckloads, which produce a low initial density. Additionally, the particles of material can reach sizes in the order of metres, which is not common in dam construction.

The investigation and results of the characterization of the geomechanical properties of the waste material from Codelco´s Andina Division is presented in this paper. In particular, characterisation of the particles and large scale shear resistance tests were carried out in an attempt to simulate the field conditions in terms of grain size distribution of the material and level of the expected loads.

1 Introduction

The mines of Codelco, Andina Division (CAD) are located in the Andes Mountains, at more than 3,700 m above sea level, just north-east of the Chilean capital Santiago. CAD extracts ore from the underground mine Río Blanco, and from the open pit mines Sur-Sur, Don Luis and La Unión, and produces copper concentrates. Currently, CAD is studying the "New Andina" Project, which will scale up the production from 72,000 tpd (tons per day) up to 230,000 tpd in the next ten years.

One of the challenges that CAD will face during the expansion is the location of the waste dumps, because of the steep terrain and scarcity of space. Given these conditions, it is envisaged that the waste dumps of "New Andina" will become enormous structures, some of which will contain over 1000 Mt of material and will reach frontal heights of up to 900 m. There is no precedent in the world for waste dumps of these dimensions.

The waste material of CAD was characterised from the geotechnical point of view. Particle size distribution, grain quality, and shear resistance was studied. For this investigation a large-scale triaxial cell was used, which can test specimens that are 2 m high and 1 m in diameter.

Crushing of particles is expected within the dump due to the high loads anticipated. This will contribute to a decrease in the friction angle as confining pressure increases. The permeability of the dump body will also be affected because of the crushing.

Although some doubts exist as to how representative laboratory testing is of the true field behaviour, large-scale triaxial testing has undoubtedly become a valuable tool for studying the behaviour of coarse material under very high loads. In the future, as high-altitude mine projects become more ambitious, more robust technology may be needed for rockfill testing.

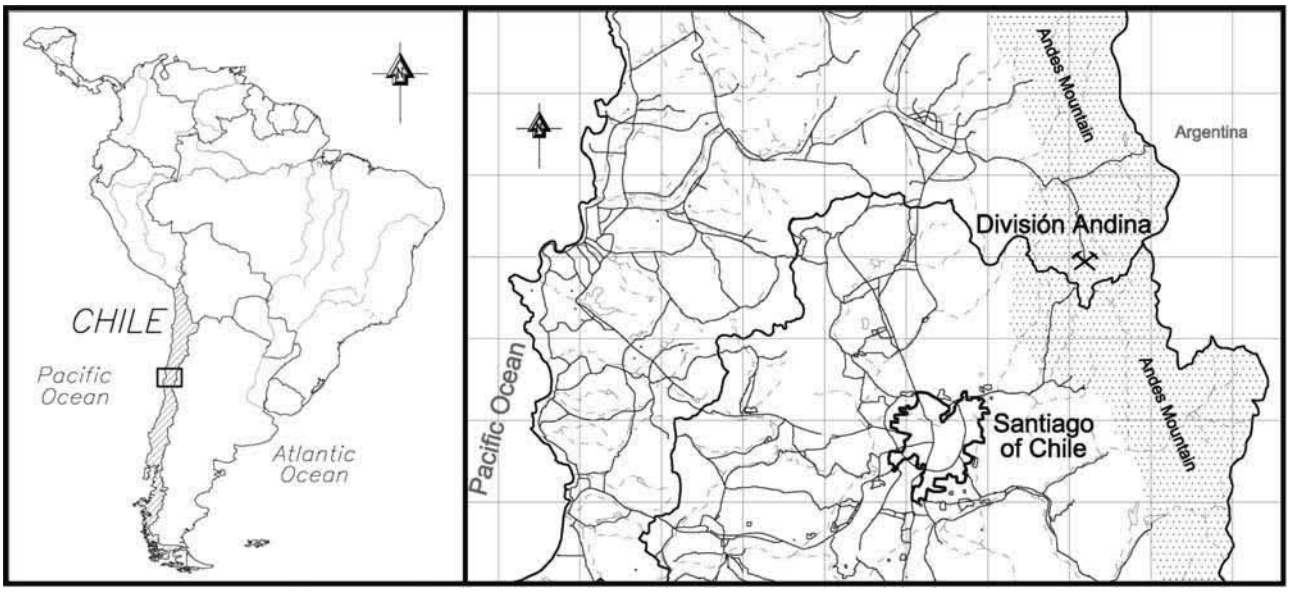

Figure 1 Map showing the locations of Division Andina of Codelco's mines

Figure 2 Andes mountains environment in Division Andina of Codelco

2 Testing plan

2.1 General

The testing programme included particle size distribution, index tests to characterise the conforming particles, and shear resistance and deformability evaluation with the triaxial test on specimens of 2 m in height and 1 m diameter. In addition, the crushing of particles due to the applied shear stress was studied. The crushing phenomenon does not only affect the resistance and deformation of the material at the different stress levels, but is also closely related to changes in the particle size distribution and consequently, to the permeability.

2.2 Grain size analysis

Determination of particle size distribution of waste material was performed by analysing a representative sample (large scale procedure). The sample, composed of 50 t of waste material, was obtained directly from blasting to avoid the 'rehandling' of the sample which could lead to a loss of material, especially the finer fraction. The processing of this type of sample often requires both laboratory and field work. The largest blocks had to be individually measured (dimensions and weight) in the field in order to include these in the particle size distribution analyses, and the remainder was taken to the laboratory.

The maximum size and particle size distribution determine the quantity of inter-granular contact points, and control the distribution and magnitude of the particle loads; thus it greatly influences the shear resistance and deformability of the material. Well graded materials (high uniformity coefficient, Cu) reach higher densities and their grains have a higher amount of contact points. Therefore they distribute the particle stresses in a better manner, reaching higher shear resistance compared to materials of the same origin but poorly graded.

2.3 Index tests for the evaluation of particle resistance

Individual resistance of the particles also affects the shear resistance and compressibility of materials. If the particle resistance is high compared to the confining stresses, it is expected that dilatancy in dense materials helps to increase the shear resistance. On the other hand, particles with lower resistance would tend to break down, diminishing the dilatancy effect and consequently decreasing the shear resistance of the rockfill. For this project, particle tests were conducted to estimate the particle resistance, such as simple compression on rock core UCS, resistance by abrasion and impact in the Los Angeles machine (ASTM C 535), soundness by use of sodium sulfate (ASTM C 88), and specific gravity of solids.

2.4 Evaluation of shear strength and deformation modulus

To evaluate the shear resistance, large-scale triaxial equipment was used. A series of five points and a series of three points of triaxial tests CID (Isotropically-consolidated and drained) were performed. The samples were prepared with a dry density of 18.5 kN/m^3 (initial void ratio of 0.46), and fully saturated before testing. This density corresponds to a loose state of the material, representing the density obtained when the material is dumped from the trucks. For the series of five points the specimens were prepared with a scaled particle size distribution, “parallel” to the field particle size distribution. For the three points series the specimens were built with a “truncated” particle size distribution sample. The maximum particle size in the specimens was 200 mm. The samples were initially isotropically-consolidated to confining stresses between 0.1 MPa and 2.5 MPa and then loaded under controlled stress condition.

2.5 Particle breakage evaluation

A particle size distribution (PSD) test was performed on each sample after testing in the triaxial cell in order to evaluate the grain breakage. Comparison of the pre and post PSD test results allowed for the observation of changes in the particle size distribution as a consequence of the triaxial shear stresses applied.

2.6 General characteristics of the triaxial equipment and the specimens configuration

The triaxial equipment used for this work belongs to the IDIEM Laboratory of the Universidad de Chile in Santiago. The equipment allows for testing specimens of 2 m high and 1 m in diameter, under controlled stress conditions, and confining pressures up to 2.5 MPa (Figure 3 and 4).

The triaxial cell is bottle shaped and buried below ground level. The lower part of the chamber is 1.7 m in diameter and 2.7 m high. The reaction frame and the system in general, are designed to apply loads up to 2000 t.

The volumetric changes, during the test, are calculated by controlling the mobilised water volumes to and from the cell, measuring weight changes through a connected pressurised water tank. The equipment has a data acquisition system, and a control panel, that allows for monitoring flows and applied pressures during the testing.

The strains are measured externally by three linear variable displacement transducers (LVDT).

Each specimen was prepared in the laboratory, compacting eight consecutive layers in total. The material for each layer was prepared (PSD), homogenised, and homogeneously placed before compacting. Each layer was compacted manually using a heavy rod. All the specimens were prepared at the same dry density of 18.5 kN/m^3 (0.46 initial void ratio).

The mould for the specimen preparation consists of three independent parts that make up the cylinder. Natural rubber membranes, 5 mm thick, were used for containing the specimen. These were vacuum fitted inside the cylinder. A non-woven geotextile was placed as an interface between the material and both caps, at

the top and bottom of the specimen. All specimens were covered by a second natural rubber membrane to avoid water infiltration in case the inner membrane was punctured. The second membrane was placed on the specimen after the mould was withdrawn. Two additional membranes were necessary for the higher confining pressure tests.

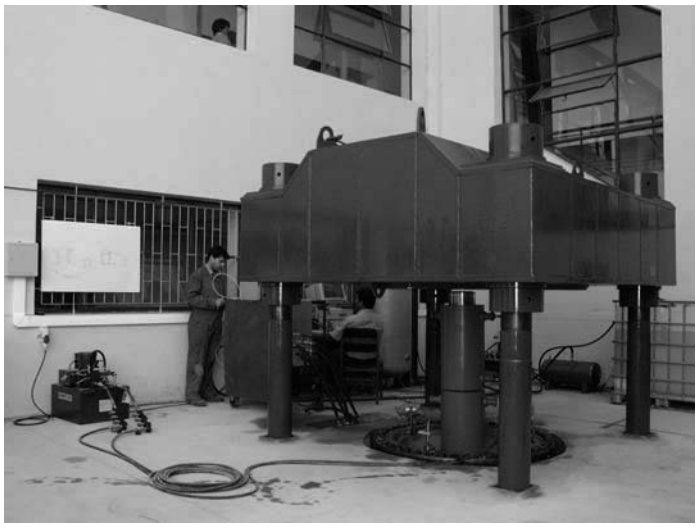

Figure 3 Triaxial equipment at IDIEM laboratory

Figure 4 Assembly of a specimen in the triaxial chamber

Once the specimen was fitted inside the chamber, a vacuum of 0.03 MPa (30 kPa) was applied to stabilize it during the cell filling. Saturation was achieved using de-aired water, after supplying CO_2 for 24 hours. Saturation over 95% was verified in all the cases.

The load was applied by increments of 2-5 t, registering the volumetric changes and axial deformation for at least fifteen minutes before applying the next load (assuring a steady state was reached in all cases). The process finalised when reaching 20% of axial strain.

The registered deviation stress was corrected to account for the resistance offered by the rubber membrane following the ASTM4767 recommendations. The membranes used were 5 mm thick with an elastic modulus of 17.4 MPa. Other corrections, related to the weight of the cap and the sample itself, were introduced.

3 Characteristics of the tested material

The physical characteristics of the representative sample and the scaled samples are described below:

3.1 Field sample

The investigated CAD waste material comes mainly from porphyry rock and granodiorite, which can be described as strong to very strong rocks. The UCS of the porphyry and the granodiorite is in the order of 130 MPa and 120 MPa respectively. The grains are angular shaped and strong. Small losses were attained in the Los Angeles machine test (15.8%) and in the soundness test using sodium sulfate (0.6%). The specific gravity was defined as 2.7 and 2.8 for over and under No. 4 sieve (US standard = 4.75 mm) respectively.

The field sample appears to be well graded, with a 'typical' maximum size (D_{100}) of 406 mm, medium size (D50) of 76 mm and only 8% corresponds to sand and fine material. The in situ dry densities, tested over dump platforms using the water replacement method, were in the range of 18 to 19 kN/m^3. The natural moisture content ranged from 5.7 to 7.3%.

Figure 5 presents the particle size distribution as displayed on the typical range of mine waste materials. The main characteristics of the field sample are presented in Table 1.

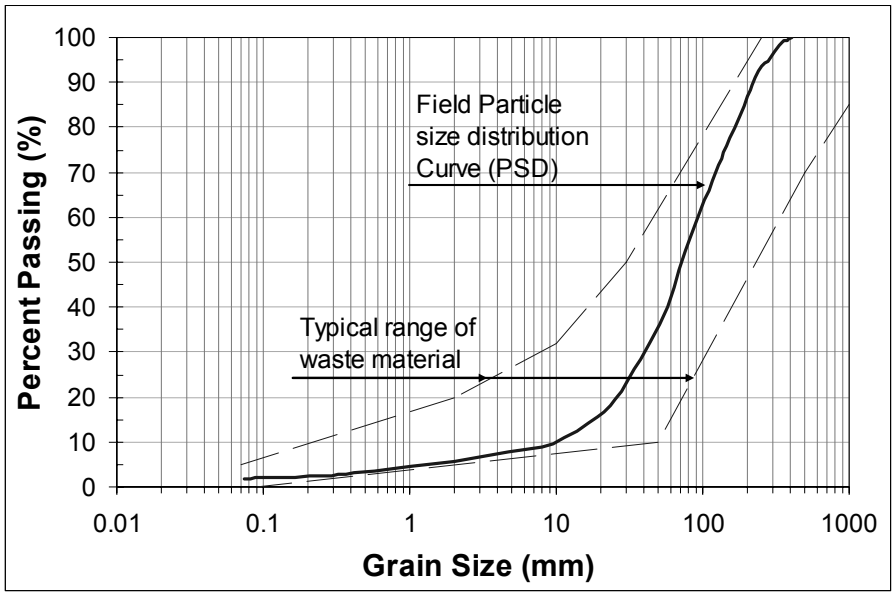

Figure 5 Particle size distributions of the field sample and typical range of waste materials

Table 1 Characteristics of CAD waste material

% passing sieve N°4-N°200	8-2%
D_{10}	10 mm
D_{30}	42 mm
D_{60}	90 mm
D_{100}	406 mm
Cu; Cc	9; 2
Gs [Above/Below sieve N° 4]	2.7 / 2.8
Soundness by sodium sulfate [% losses]	0.6
Abrasion Los Angeles [% losses]	15.8
UCS [MPa]	120-130

3.2 Scaled sample

Two ways for scaling the sample were used. The first method considered was a particle size distribution (PSD), "parallel" to the field sample, in log scale. This method ("parallel" scaled) allows the sequence of the grain sizes from the original sample to be maintained, giving a true scaling of the material (Lee, 1986, Verdugo and Gesche, 2003). Based on the equipment characteristics, a maximum particle size of 200 mm was defined for the construction of the testing specimens. This allows for a ratio of 1 to 5 between the maximum particle size and the diameter of the specimen (as suggested in literature). In the second method the field PSD was scaled by simply scalping sizes over 200 mm ("truncated" scaled).

Figure 6 shows the PSD of the field sample, and the PSD of the scaled samples. The main characteristics of the scaled curves are shown in Table 2.

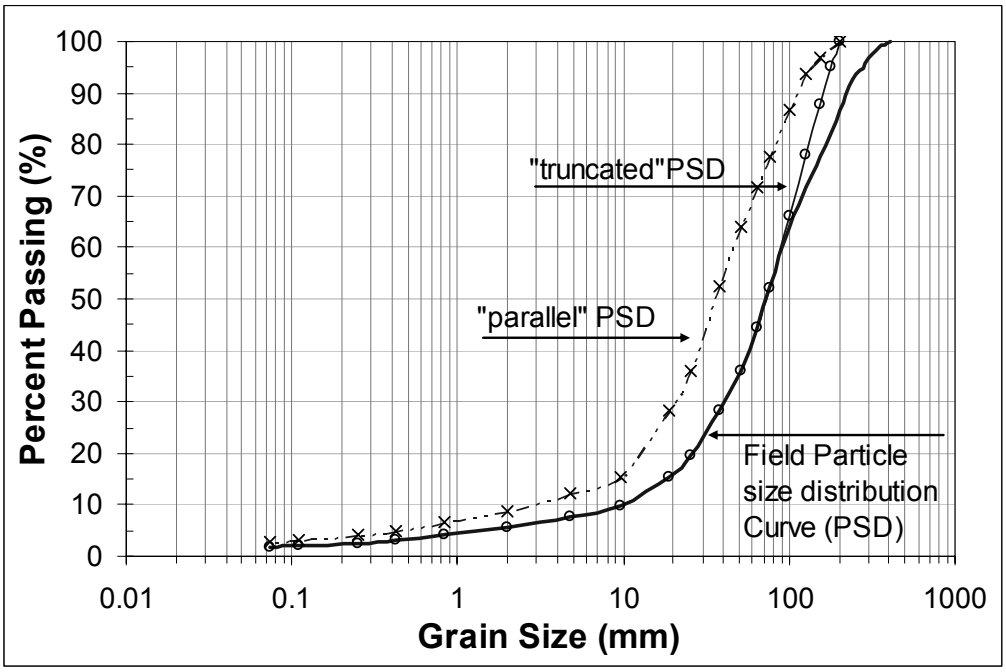

Figure 6 Particle size distributions: field sample curve, "parallel" curve and "truncated" curve

Table 2 Characteristics of the scaled particle size distributions

Characteristics of PSD	Parallel scaled	Truncated scaled
% passing mesh N°4-N°200	11-3%	8-2%
D_{10}	4 mm	10 mm
D_{30}	19 mm	41 mm
D_{60}	50 mm	89 mm
D_{100}	200 mm	200 mm
Cu; Cc	16; 3	9; 2

4 Triaxial testing results

4.1 Material behaviour and results at the ultimate state

The triaxial test results are summarised in Tables 3 and 4.

Table 3 Triaxial test results at failure – "parallel" PSD

Test	e_i	σ_3 (MPa)	σ_1/σ_3 max.	ϕ_0 (°)	ε_a (%)	ε_v (%)	Bg (%)
1	0.45	0.1	7.3	51	11	-1.9	6.4
2	0.44	0.2	6.0	47	18	-4.2	7.7
3	0.43	0.5	4.6	40	18	-5.9	9.4
4	0.39	1.0	4.4	39	15	-7.4	13.6
5	0.34	2.0	3.3	32	17	-13.1	15.0

Note: e_i=Initial void ratio after isotropic consolidation; σ_3=Confining pressure; σ_1/σ_3 = Principal stresses ratio; ϕ_o = Friction angle at origin (considering null cohesion); ε_a =Axial strain at failure; ε_v =Volumetric strain at failure. Conventional signs for strain: (-) compression, (+) expansion; Bg = Marsal particle breakage parameter (represents, approximately, the percentage in weight of particles that have suffered fragmentation).

Table 4 Triaxial test results at failure – "truncated" PSD

Test	e_i	σ_3 (MPa)	σ_1/σ_3 max.	ϕ_0 (°)	ε_a (%)	ε_v (%)	Bg (%)
1	0.44	1.0	4.5	38	21	-8.6	16.4
2	0.37	1.6	5.0	40	21	-9.3	24.1
3	0.36	2.5	4.0	36	21	-13.8	30.0

Note: e_i=Initial void ratio after isotropic consolidation; σ_3=Confining pressure; σ_1/σ_3 = Principal stresses ratio; ϕ_o = Friction angle at origin (considering null cohesion); ε_a =Axial strain at failure; ε_v =Volumetric strain at failure. Conventional signs for strain: (-) compression, (+) expansion; Bg = Marsal particle breakage parameter (represents, approximately, the percentage in weight of the particles that have suffered fragmentation).

Figures 7 and 8 present stress evolution versus axial strain for each test performed at different confining pressures. Shear strength increases fairly linearly until it reaches an axial strain close to 5%. Then, the increment rate decreases and the strength reach its maximum value at strains over 15%. For confining pressures ranging from 0.1 to 0.5 MPa, rupture peaks cannot be identified and the curves seem to tend to the maximum value with an asymptotic shape which is characteristic of loose materials.

Figures 7 and 8 also show the changes in volume with the axial strain, for each test of the two series.

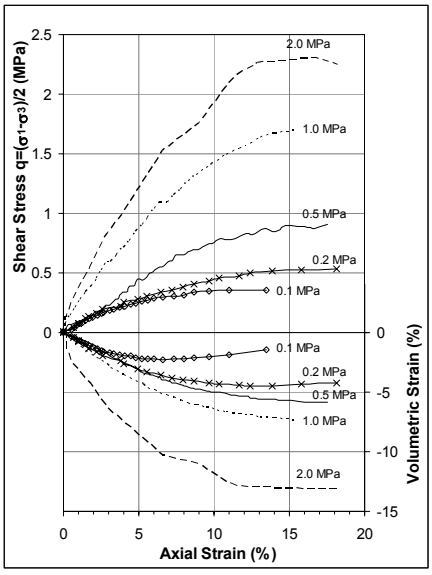

Figure 7 Shear stress and volumetric strain versus axial strain, "parallel" PSD

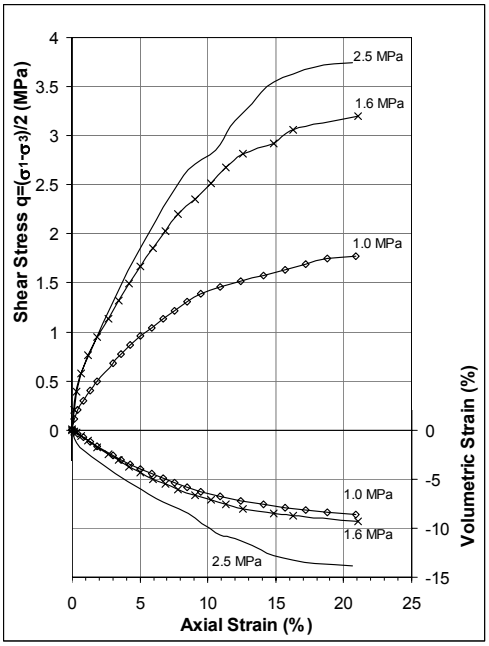

Figure 8 Shear stress and volumetric strain versus axial strain, "truncated" PSD

A contractive behaviour at the initial range of axial strain (up to 5%) is observed. Beyond that, this tendency decreases for tests performed at confinement pressures below 0.5 MPa but keeps the same trend for the tests performed at confining pressures above 0.5 MPa. This behaviour confirms low relative density used for building the specimens and, on the other hand, particle breakage occurrence which is exacerbated for the higher-stress tests. The decrease in volume is the result of the re-accommodation of grains and the crushing.

The shear strength does not have a linear behaviour when plotted as a function of the applied normal stress, as observed in Figures 9 and 10. This trend is illustrated in Figure 11 which shows that the shear strength/normal pressure ratio continues to decrease with increasing normal pressure until the normal pressure reaches 1 MPa.

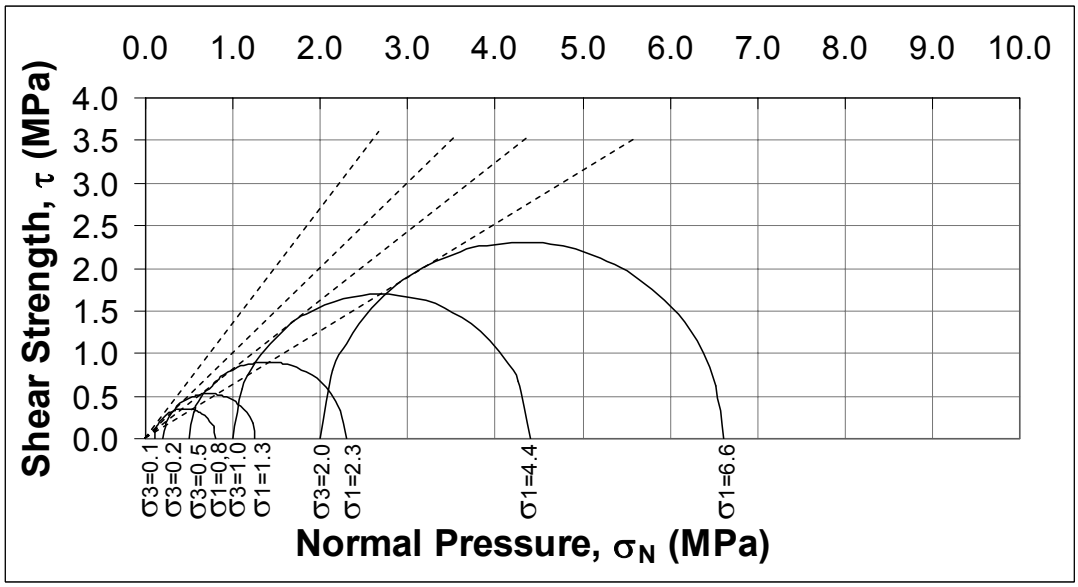

Figure 9 Mohr circles for an axial strain of 15%, "parallel" PSD case

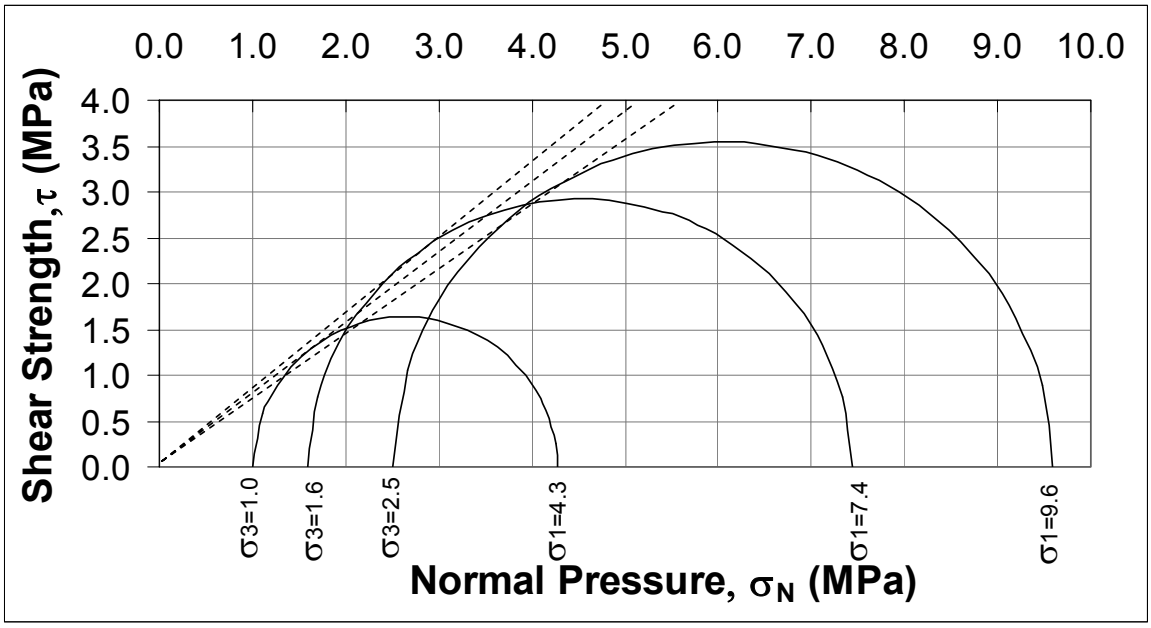

Figure 10 Mohr circles for an axial strain of 15%, "truncated" PSD case

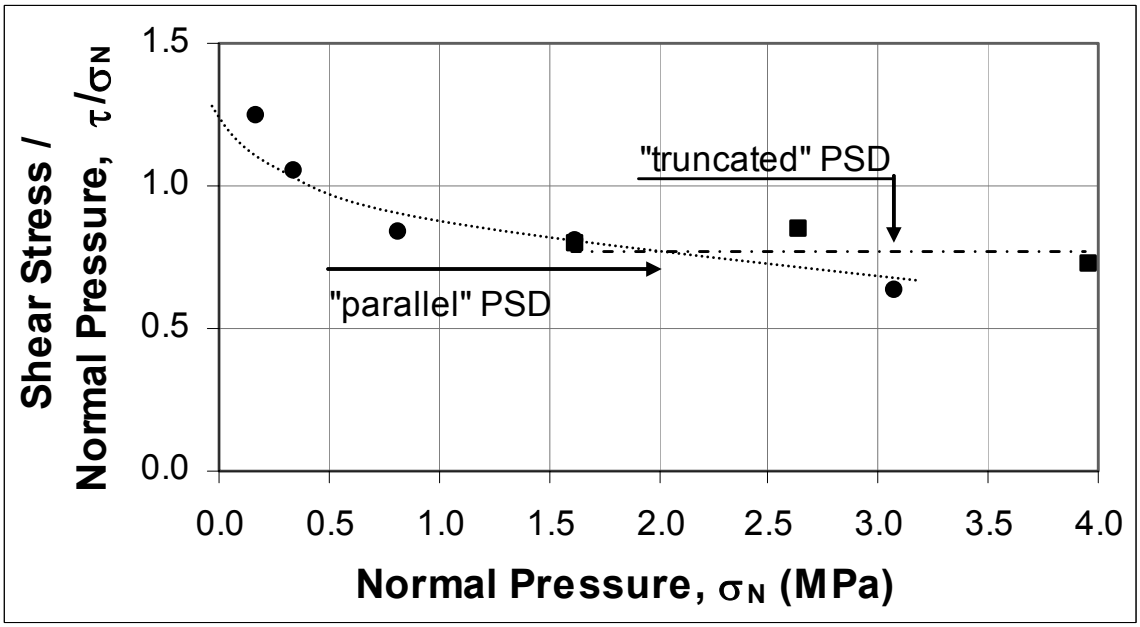

Figure 11 Variation of the shear stress/normal pressure ratio with the normal pressure

From the above, the typical reduction in the angle of friction with the increment of the confining pressure can be established. In Figure 12 this relation is presented and compared with other results published in technical literature corresponding to "quarry" materials (high angularity similar to the particle angularity of the waste), tested in 1 m^2 cross-section specimens (Marsal and Resendiz, 1975). The friction angle of the waste material varied from 51º to 32º at a normal stress range of 0.18 to 4 MPa, which correlates well with the typical range for granular materials. (Leps, 1970; Indraratna et al., 1993).

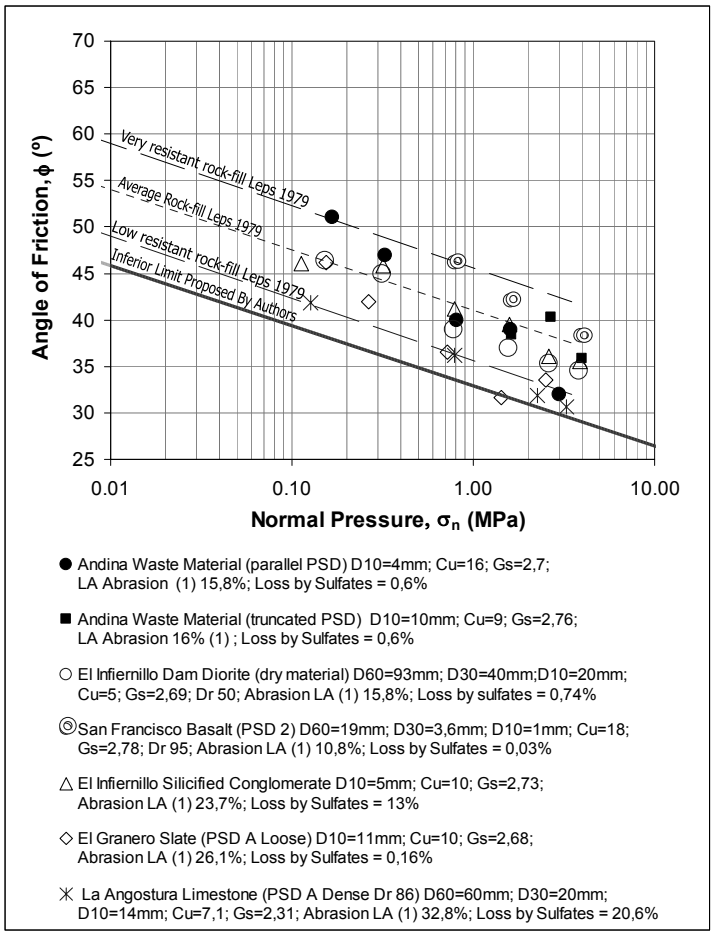

Figure 12 Variation of friction angle with normal pressure: Comparison with published results for other materials

4.2 Particle breakage

To evaluate the crushing phenomenon, the particle size distribution of the tested material was determined and compared with the pre-tested particle size distribution. These results are presented in Figures 13 and 14, where particle breakage occurrence can be visualized.

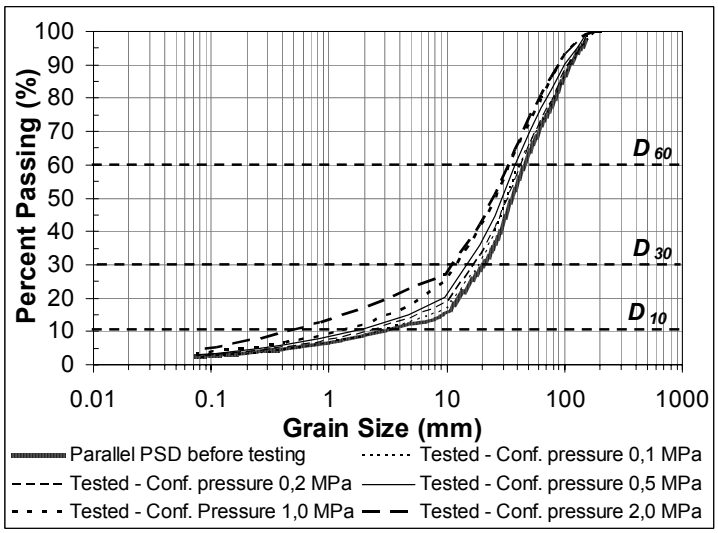

Figure 13 PSD before and after triaxial testing, "parallel" scaled samples

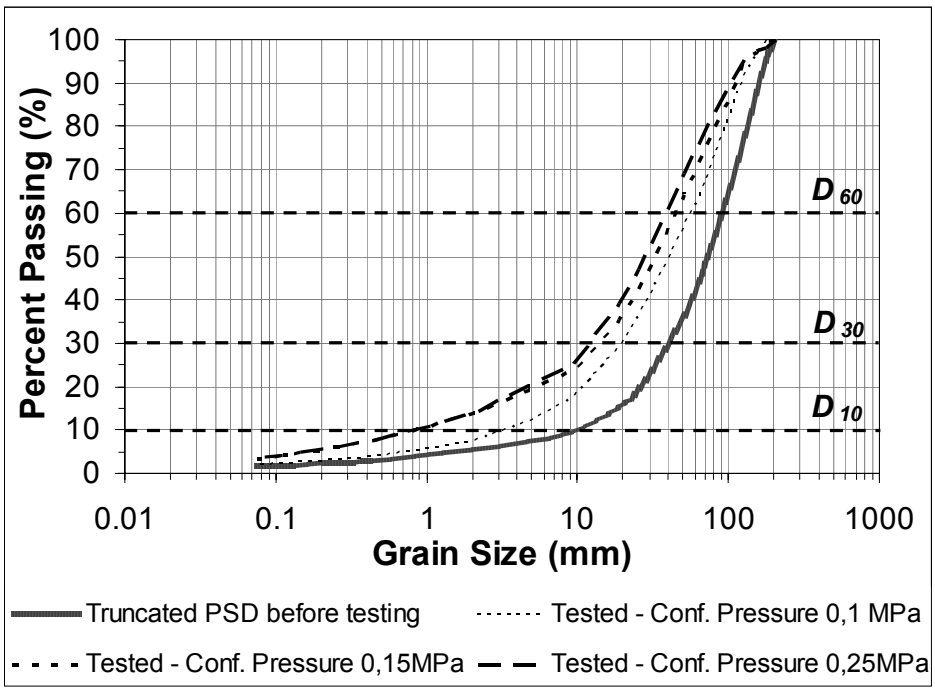

Figure 14 PSD before and after triaxial testing, "truncated" scaled samples

Variations of D_{60}, D_{30} and D_{10} are presented in Figures 15 and 16. It is observed that as the stress levels increase, the gradation of the material improves (the uniformity coefficient increases). When testing of materials with "parallel" PSDs, D_{10} varies by one order of magnitude in the pressure range studied, decreasing from 3 to 0.4 mm. For the tests using a "truncated" PSD, D_{10} had a variation of two orders of magnitude in the pressure range studied, decreasing from 10 to 0.8 mm.

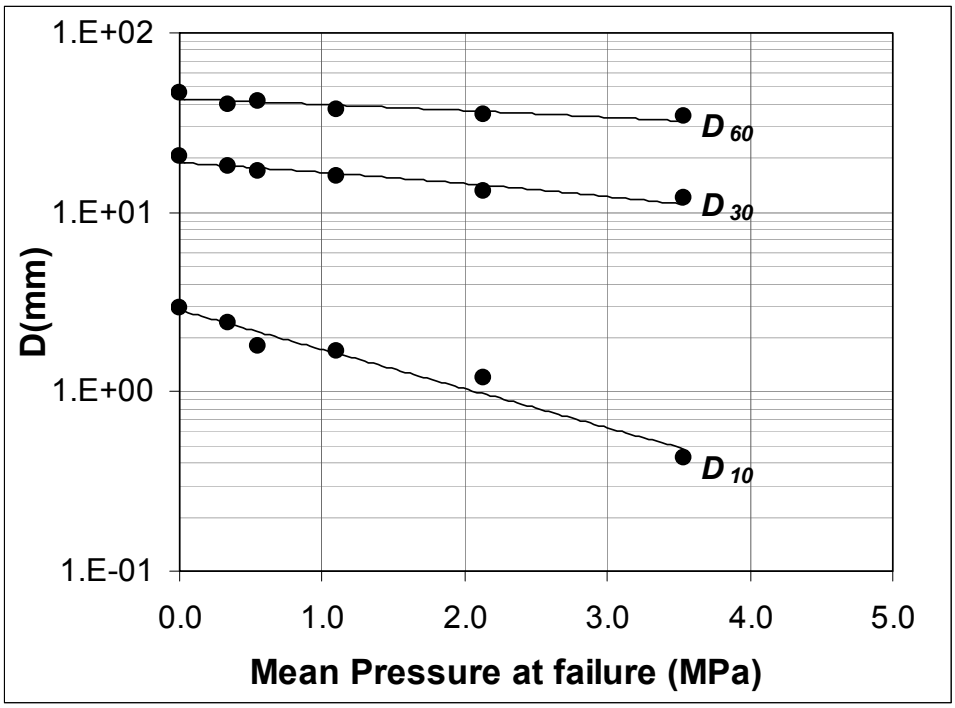

Figure 15 Variation of sizes D_{60}, D_{30} and D_{10} with the mean pressure at failure, "parallel" scaled samples

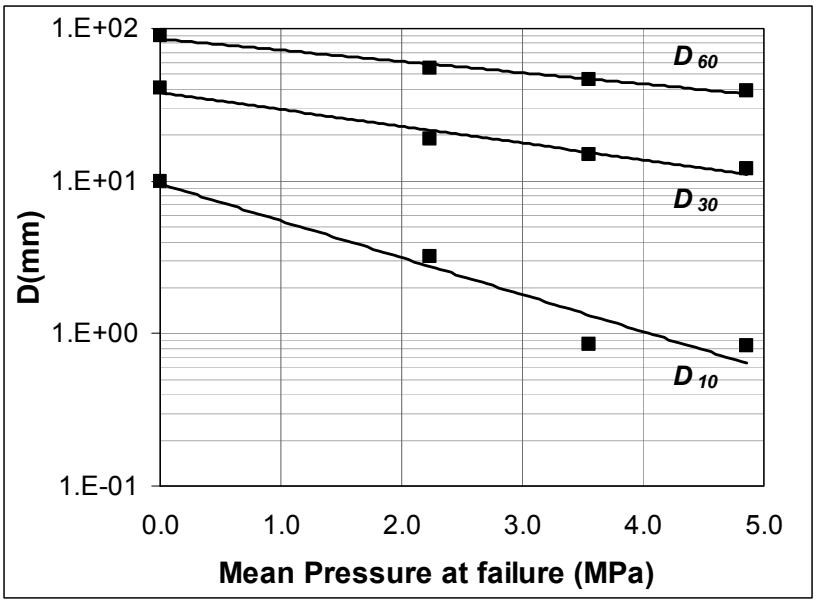

Figure 16 Variation of sizes D_{60}, D_{30} and D_{10} with the mean pressure at failure, "truncated" scaled samples

In order to quantify the grain breakage, a parameter Bg for granular materials proposed by Marsal was used. (Marsal and Resendiz, 1975). It is obtained from the differences in percentages of the retained material for each sieve between the initial and final particle size distribution curves. Addition of all these differences is equal to zero. Bg corresponds to the sum of the positive values and represents approximately the percentage in weight of the particles that have suffered fragmentation.

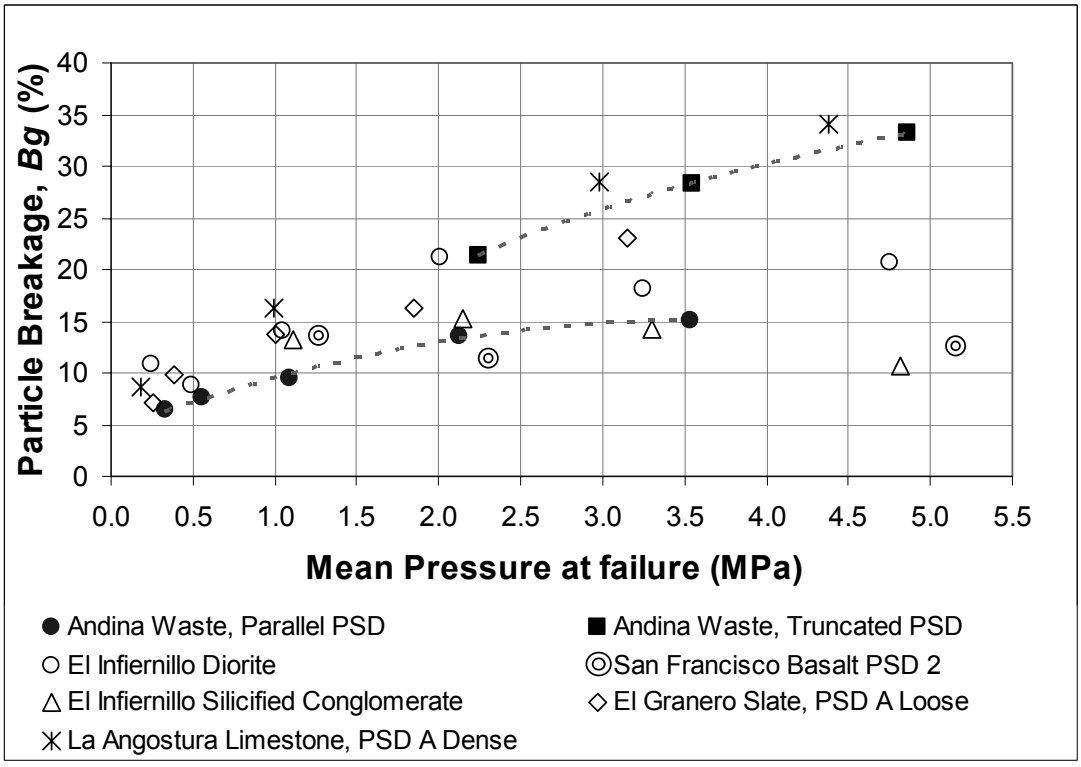

Figure 17 Bg Parameter variation

For tests performed with material of "parallel" scaled PSD, the Bg parameter varied approximately linearly between 6 and 14% for stresses between 0.3 and 1 MPa and increase with a lower rate for higher stresses. The previous may suggest that above some stress level, the particles already crushed by their internal weakness zones, shift to a phase where edge breaking and sand and fines generation is predominant, which is not reflected on the Bg value. For tests performed with "truncated" PSD material, the Bg parameter increased near-linearly with the pressure within the range of stress studied (Figure 17) and the Bg values are higher compared to those obtained for the "parallel" PSD sample. This may be due to the higher content of coarse particles that result from cases of "truncated" scaling of the sample. Coarse particles are more susceptible to breakage.

4.3 Shear resistance envelope

The Mohr resistance envelope has been defined using a potential equation to adjust the results, where A and B are material constants (Charles and Watts, 1980).

$$\tau = \mathbf{A}\ \sigma_n^{\ b} \tag{1}$$

In the above equation τ is the shear strength and σ_n is the normal stress, while A and b are material constants for which the values are estimated based on the results of triaxial tests.

Figure 18 presents the resistance envelope, which has been evaluated up to an effective normal pressure of 1.5 MPa and later on, evaluated up to 4 MPa considering a 15% of axial strain as the failure criteria. For comparison, this figure also includes the envelopes corresponding to the materials investigated by Marsal (Marsal and Resendiz, 1975). Table 5 lists A and b values for all the cases. Materials with higher resistance generally present higher values of A. The b parameter determines the curvature of the resistance envelopes. Hence materials with higher resistance also present higher values of b.

Table 5 A and b failure envelope parameter

Material	A	b
Andina Waste, "parallel" scaled PSD	0.84	0.78
Andina Waste, "truncated" scaled PSD	0.86	0.90
El Infiernillo Dam Diorite	0.81	0.86
San Francisco Basalt	0.99	0.83
El Infiernillo Silicified conglomerate	0.85	0.88
El Granero Slate	0.72	0.82
La Angostura Limestone	0.70	0.87

In the range of low stresses, up to 1 MPa approximately, the material develops a high resistance, with the resistance envelope lying between the El Infiernillo Diorite and the San Francisco Basalt (Marsal, 1980) both igneous materials with hard grains. Nevertheless at higher stress levels, the material scaled with "parallel" PSD presents a lower resistance than Infiernillo Diorite and San Francisco Basalt due to the more pronounced curvature of the envelope. The material scaled by "truncated" PSD maintains higher resistance in comparison.

Therefore, the evaluated shear resistance equations would be as follows:

$$\tau = 0.84\ \sigma_n^{0.78}\ \text{(MPa) when testing the Parallel PSD} \tag{2}$$

$$\tau = 0.86\ \sigma_n^{0.90}\ \text{(MPa) when testing the Scalped PSD} \tag{3}$$

High resistances (high internal friction) identified in the laboratory for very low stresses, apparently do not correlate well with the observations in the field about the waste deposit behaviour. In practice, the angle of repose of loose material (overturned by trucks) reaches approximately 38°. During a seismic event, mobilisation of superficial material is frequent, denoting that materials in the slope faces are near their

equilibrium limit. This situation may be related to the construction method which induces the orientation of particles at the slope face, in the same direction of potential shallow failure surfaces.

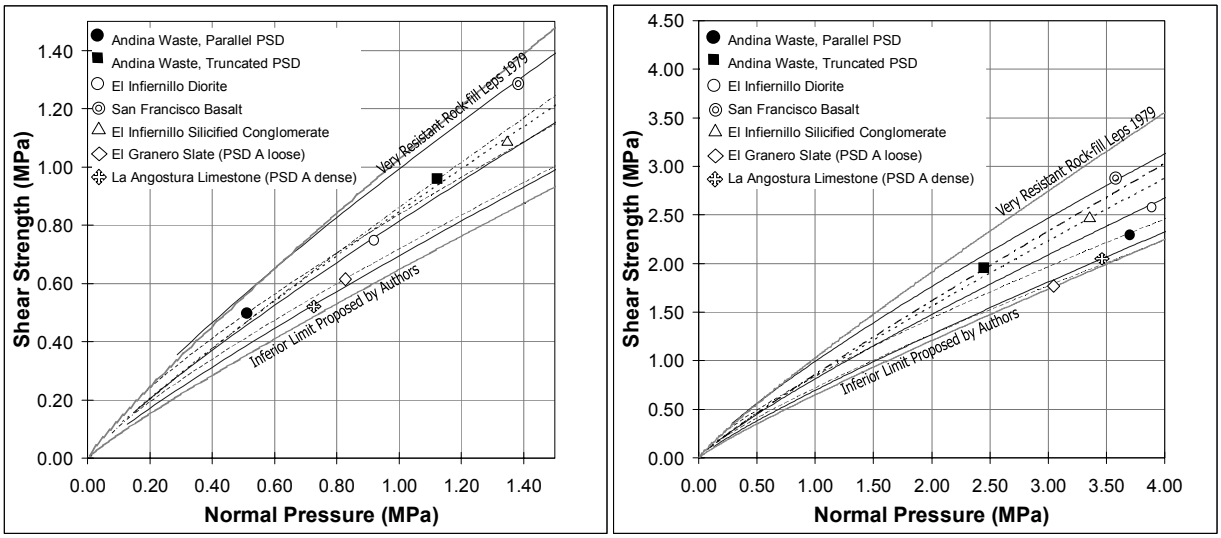

Figure 18 Andina waste shear resistance envelope and comparison with other material envelopes (as from quarry and angular)

Consequently, adjustment of the resistance envelope for low stresses is recommended for design. A resistance which is proportional to the normal pressure and is determined by the internal angle of 40° (internal friction angle two degrees more than the rest angle obtained by over-turning) appears as recommendable.

The resulting resistance envelope band is presented in Figure 19. The shear resistance differences found between "parallel" and "truncated" samples may reflect that, in the case of hard constitutive particles, coarser materials exhibit higher resistance. Nevertheless, a scaling effect should not be excluded and needs to be further investigated. The author considers that a ratio diameter of 1 to 5 may be insufficient for these kind of sizes which would be more critical in the case of the "truncated" PSD which contains a greater proportion of coarse particles.

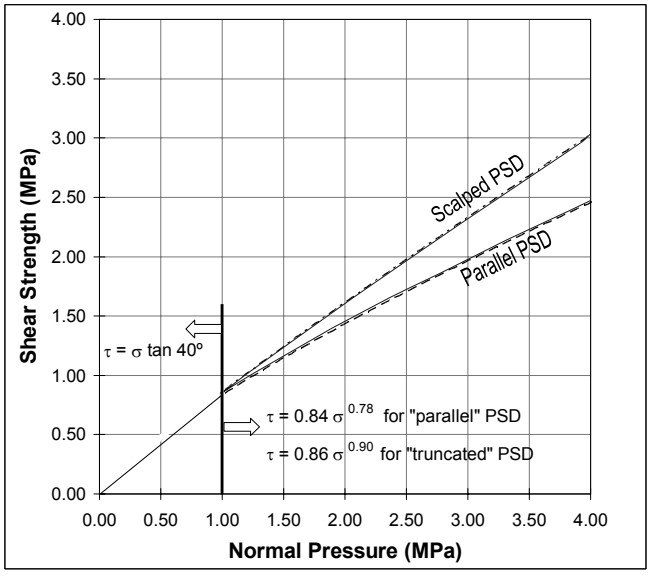

Figure 19 Failure envelopes

4.4 Modulus of deformation

The triaxial test results were used to establish the stress-strain characteristics of the material. The instantaneous slope of the curves, or tangent modulus Et, can be estimated by the following expression (Duncan and Chang, 1970).

$$E_T = Ei \cdot \frac{\left(1 - R_f \cdot (\sigma_1 - \sigma_3)\right)^2}{\left(\sigma_1 - \sigma_3\right)_f} \tag{4}$$

Where:

Ei = Initial tangent modulus = $k\ p_a\ (\sigma_3 / p_a)^n$

Rf = Failure Relation = $(\sigma_1 - \sigma_3)_f\ /\ (\sigma_1 - \sigma_3)_{ult}$

k = Modulus factor; pa = Atmospheric pressure expressed in the same units of E_t; n = Exponent that determines the variation of Et with σ_3.; $(\sigma_1-\sigma_3)_f$ = Deviator stress at failure; $(\sigma_1-\sigma_3)_{ult}$ = Ultimate stress-difference value when evaluated over the Duncan transformation curve.

The initial tangent modulus Ei and the Rf value, have been evaluated from the stress-strain curve of the Duncan transformation for each test.

Figure 20 relates the initial tangent modulus with the confining pressure, and parameter k and n can be established from there. Rf = 1 has been obtained for both test series, of "parallel" and "truncated" scaled PSD samples.

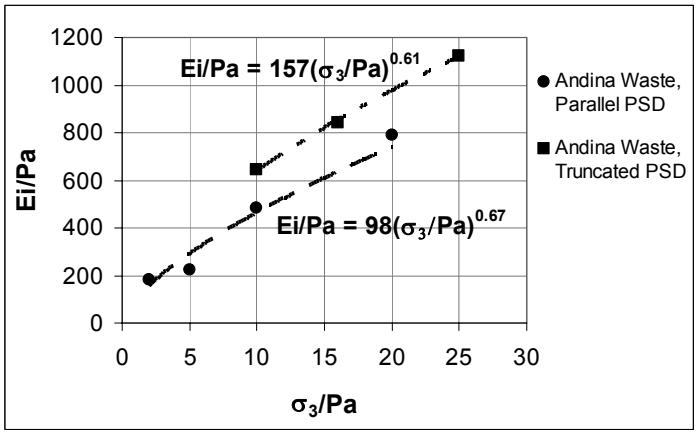

Figure 20 Relationships between the initial tangent modulus and the confining pressure

The k values of 98 and 157, obtained for the "parallel" and "truncated" materials respectively, correspond to the Young modulus for σ'_3=0.1 MPa. These values differ from typical values for granular materials, especially rock-fills (200 to 600). However it must be emphasised that there are few reported values based on large-scale tests such as these carried out for this research; especially those reported for loose materials. Generally the studies that can be found as reference are focussed on civil construction, where the materials in general receive an important degree of compaction to limit their deformability in the short and long term.

4.5 Additional considerations

Based on the volumetric changes measured during the load application, void ratio versus the applied stress was calculated, as shown in Figure 21. The relationships have a bi-linear shape in both, isotropic consolidation and failure cases. The slope of the curve is accentuated when overpassing certain value of pressure. These slope changes are attributed to the particle breakage that favours the change of the PSD towards a state of better gradation and greater density. It is expected that this slope change is reverted at

some point where the material is able to establish a stable skeleton and therefore the particle breakage starts to decrease. Tests at decidedly greater stresses would be necessary to establish this condition.

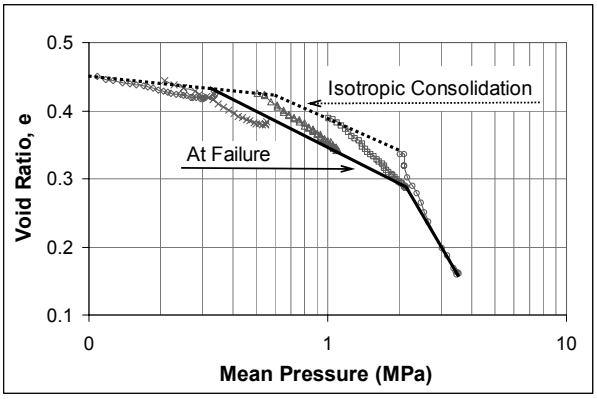

Figure 21 Voids ratio versus Mean pressure, "parallel" PSD

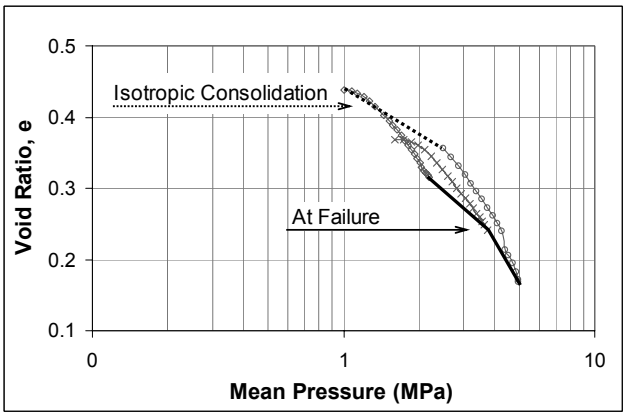

Figure 22 Voids Ratio versus Mean pressure, "truncated" PSD

5 Conclusions

The considerable development of the large-scale copper mining industry is requiring the construction of enormous waste deposits. In mountain range topographies, these deposits can reach hundreds of metres of frontal height, thus the detailed knowledge of the geomechanical characteristics of the constituent material has become indispensable for its design.

Generally, the experiences in characterization of coarse granular materials have been developed in relation to projects for construction of rock-fill dams, where the dam heights are considerably lower than those which are currently being planned for Chilean mountain mine deposits.

Codelco's Andina Division has carried out important advances in the characterization of their waste materials, aiming at proper design of such deposits. This work represents a great contribution and reference for the mining industry, especially if one considers the difficulty and the costs associated with the research of this type of material.

The necessity of equipment that allows for the evaluation of granular materials under high pressure is identified. The current equipment available in laboratories has generally been designed for studying civil construction applications and cannot simulate, to a desirable range, the stress states that can be present in mining deposits located in the mountains.

The stability analyses of dumps of granular material and significant heights must consider the decrease of the internal friction angle with the normal effective pressure. Typically, the resulting potential failure surfaces would tend to develop further from the face of the deposit.

In the low stresses range, as those found at the face of the slopes, it is advisable to consider the shear resistance proportionally to the normal pressure determined by a friction angle close to the rest angle. This condition agrees with field observations that suggest that the material is near to the limit equilibrium condition at the slope faces.

The deformation modulus, estimated from the test results in this work, are low in comparison with typical values reported in technical literature for granular materials especially for rock-fills, for this reason it will have to be judged with care.

The evaluation of particle breakage (crushing) and changes in void ratio with the mean pressure indicates that high pressures would lead to PSD changes, i.e. sand and fines generation, and to a decrease of the permeability. Nevertheless, it is estimated that breakage and re-accommodation of particles must stop at some stress level on which the material is able to establish a stable skeleton with a high resistance. Higher-stress tests would be desirable to establish this stress level and to predict adequate densification and effective loss of permeability of the material, to the expected stress ranges.

Acknowledgements

The authors gratefully acknowledge the permission of Codelco Division Andina to publish this paper.

References

ASTM C 535-96 Standard Test Method for Resistance to Degradation of Large-Size Coarse Aggregate by Abrasion and Impact in the Los Angeles Machine.

ASTM C 88-05 Standard Test Method for Soundness of Aggregates by Use of Sodium Sulfate or Magnesium Sulfate.

ASTM D 4767 Standard Test Method for Consolidated Undrained Triaxial Compression Test for Cohesive Soils.

Charles, J.A. and Watts, K.S. (1980) The influence of confining pressure on the shear strength of compacted rockfill. Geotechnique 30, No. 4, pp. 353-367.

Duncan, J.M. and Chang, C-Y. (1970) Nonlinear analysis of stress and strain in soil, Journal of the Soil Mechanics and Foundations Division. ASCE, pp. 1629-1653.

Indraratna, I., Wijewardena, L.S.S. and Balasubramaniam, A.S. (1993) Large-scale triaxial testing of Greywacke rockfill, Geotechnique 43, No. 1, pp. 37-51.

Lee, Y. (1986) Strength and deformation characteristic of rockfill. PhD thesis, Asian Institute of Technology.

Leps, T. (1970) Review of shearing strength of rockfill. Journal of Soil Mechanics and Foundation Division, ASCE. Vol. 96, SM4, pp. 1159-1170.

Marsal, R.J. (1980) Contribución a la mecánica de medios granulares. Comisión Nacional de Electricidad, Mexico, D.F.

Marsal, R.J. and Resendiz, D.R. (1975) Presas de Tierra y Enrocamiento. Mexico. Ed Limusa, pp. 237-239.

Verdugo, R., Gesche, S. and De La Hoz, K. (2003) Metodología de Evaluación de Parámetros de Resistencia al Corte de Suelos Gruesos. XII Panamerican Conference on Soil Mechanics and Foundation Engineering, MIT. USA. Vol. 1, pp. 691-696.